Short communication

High strength-ductility of heterogeneous sandwich Mg–Y alloys produced by high pressure torsion

Xuefei Chen [a,b], Lirong Xiao [c,*], Yi Liu [c], Mengning Xu [c], Tao Xu [c], Bo Gao [c], Zhaohua Hu [d], Hao Zhou [c,**]

[a] State Key Laboratory of Nonlinear Mechanics, Institute of Mechanics, Chinese Academy of Sciences, Beijing, 100190, China
[b] School of Engineering Sciences, University of Chinese Academy of Sciences, Beijing, 100049, China
[c] Nano and Heterogeneous Materials Center, School of Materials Science and Engineering, Nanjing University of Science and Technology, Nanjing, 210094, China
[d] Ansteel Beijing Research Institute Co., Ltd, Beijing, 102209, China

ARTICLE INFO

ABSTRACT

Due to unique precipitation behavior, magnesium-rare earth (Mg-RE) alloys exhibit excellent strength. However, owing to the blocking effect of solid solute atoms on the slipping of dislocations, the plasticity of Mg-RE alloys becomes poor. In this work, HPT followed by solution and aging treatment is used to produce laminate heterogeneous Mg–Y alloys by sandwiching a hard layer and two soft layers. Specially, the interface transition region shows a gradient distribution of Y concentration and precipitation. The sandwich Mg–Y alloy attains an enhanced strength-plasticity synergy.

Mg and its alloys possess great potential applications in aerospace, automotive, electronics and biomedical industries, due to their high specific strength, good stiffness and excellent biocompatibility [1–3]. However, low strength [4] and poor plasticity [5] are the main limits for their comparative applications. In order to improve the strength of Mg alloys, magnesium-rare earth (RE) alloys have been developed, which provide additional strengthening by nano-scaled precipitations and interfacial segregation [6–8]. He [9] reported an age hardened Mg-Gd-Y alloy, enhancing from 130 MPa to 239 MPa. However, due to the blocking effect on dislocation slip, uniform elongation of most Mg-RE alloys is reduced drastically by precipitations [10,11]. Thus, a question arises on how to attain an enhanced strength-plasticity synergy in Mg-RE alloys.

Heterogeneous materials are a class of new developed materials with unprecedented mechanical properties [12–16]. The typical microstructure in heterogeneous materials is that there always exist various zones with dramatically different strengths, while the geometry and the sizes of the zones might vary widely [12]. People tried to produce a hetero-structure with coarse grains embedded in fine grains in Mg-RE alloys [17]. However, the strength contrast between the coarse and fine grains was diminished after aging treatment. Because the prior soft coarse grains were significantly strengthened by the nano precipitations,

such as β′ and γ″ [18,19]. Thus, it is difficult to design heterogeneous alloys only in a homogeneous Mg-RE alloys, which has been successfully achieved in pure Ti [13]. Laminated (or sandwiched) structures can be another strategy to produce heterogeneous Mg-RE alloys. While, the interface bonding of laminated heterogeneous Mg-RE alloys becomes another challenge. Wu [20] reported a laminate heterogeneous Mg/Al alloy by accumulated roll bonding (ARB); Unfortunately, the interface with lots of oxides results in poor mechanical properties.

In this work, we fabricated a laminate structure with a Mg-11 wt% Y layer sandwiched between two Mg-5 wt.% Y layer via high pressure torsion (HPT) by utilizing two principles: (a) Dramatically different ageing hardening effect between Mg–5Y and Mg–11Y after the same ageing treatment. It is reported that the aging hardening response of binary Mg–Y alloy is remarkable when the Y concentration in the alloy is at or above 8 wt % and the aging treatment is carried out at a temperature close to 200 °C [2]. (b) High pressure torsion can fabricate sharp interface [21] for Mg-RE alloys, compared with ARB, which is generally used in other heterogeneous laminate alloys [22,23]. Hence, using this approach, we can produce a sandwich structure with sharp and well-bonded interface. The mechanical properties of sandwich heterogeneous Mg–Y alloy are investigated and the underlying mechanism is explored. This study has a great significance for designing and

* Corresponding author.
** Corresponding author.
E-mail addresses: xiaolr620@126.com (L. Xiao), hzhou511@njust.edu.cn (H. Zhou).

preparation of heterogeneous Mg alloy.

The alloy ingots were two kinds as-cast Mg alloys: Mg-5 wt. % Y and Mg-11 wt % Y. The ingots were solution treated at 500 °C for 12 h and quenched to room temperature in the furnace. Mg–5Y and Mg–11Y plates were punched into Ø10 mm disks and ground to three groups of thickness: 0.8 mm, 1.6 mm and 3.2 mm. Then, the samples were fabricated as Table 1. Fig. 1a schematically illustrates the procedure of sample processing. The total initial thickness of three samples disks were around 3.2 mm so that sufficient thickness reduction (~69%) after processing can be achieved to form strong interfacial bonding. The samples were polishing and ultrasonic cleaning before sandwiching the disks together. HPT was applied at room temperature with 1 GPa for 10 revolutions at 1.5 rpm to obtain more homogeneous deformation along the radius direction.

The HPT samples were solution treated at 500 °C for 12 h and quenched to room temperature in the furnace. Then, isothermal aging was implemented at 200 °C in silicon oil for 128 h. Scanning electron microscope (SEM) and transmission electron microscope (TEM) samples were cut from cross section of the aged sandwich Mg–Y. SEM samples were ground using 320, 600 and 1200 grit sand papers, and polished to mirror on polish cloth using Al_2O_3 solution. Then they were etched in 5% nitric alcohol solution. Samples for transmission electron microscopy (TEM) analysis were prepared in a standard way: machining 3 mm diameter foils and then ion-milling the foils until a central perforation was formed [24]. The morphology of cross section of aged sandwich Mg–Y was investigated by using SEM operating at 20 kV. TEM samples were cut from the interface of cross section by focused ion beam (FIB). High-angle annular dark-field (HAADF) study was performed in a FEI Titan G2 60–300 TEM with probe-spherical aberration performed at 300 kV, equipped with electron dispersive X-ray spectroscopy (EDS). Dog-bone shaped specimens with a gauge length of 1.8 mm and width of 1 mm were cut from the aged HPT samples for tensile test [25,26]. The uniaxial tensile testing was performed on a walter + bai mechanical testing machine (LFM-20kN) with a strain rate of $2 \times 10^{-4}\ s^{-1}$ at room temperature. Vickers microhardness tests of the cross section of aged sandwich Mg–Y were performed under 100gf loading for 15 s at a MATSUZAWA-VMT-7S tester. At least 10 indentations were used to calculate the mean value and standard deviation.

Fig. 1b shows the cross-sectional morphology of the heterogeneous Mg–Y alloy. It displays a metallurgical bonding of the interfaces between Mg–11Y and Mg–5Y layers without oxides. The interfaces are not straight and the thickness of Mg–11Y in the middle layer is about 200 μm. The interface structure is also characterized by TEM, as shown in Fig. 1c. It shows a sharp boundary, which is similar to the grain boundary [27,28]. Magnified images of the interface were observed marked by the yellow, blue and purple box, as shown in Fig. 1d1-d3 and the corresponding Fast Fourier transform patterns in Fig. 1e1-e3, respectively. Fig. 1d1 shows there is a transition region in the interface. Fig. 1e1 shows lots of defects such as low angle grain boundaries exist in the transition region. Some steps are observed in the interface marked by pink arrows in Fig. 1d2, and Fig. 1e2 shows these are some stacking faults. No precipitates and oxides are found near the interface, as shown in Fig. 1d3 and Fig. 1e3.

Fig. 2a is age-hardening response of Mg–5Y and Mg–11Y alloys at 200 °C. As Fig. 2a shown, before aging treatment, the hardness of Mg–11Y alloy is about 35Hv higher than Mg–5Y alloy, due to solution strengthening. After the aging treatment, the hardness of Mg–5Y alloy always keeps at the same level just with slight fluctuation. While, for

Mg–11Y alloy, the peak hardness value is ~135Hv and about 70Hv higher than Mg–5Y alloy after aging for 128 h, which is mainly due to aging hardening besides solution strengthening. Fig. 2b shows the Vickers hardness value across the area shown in Fig. 2c. The hardness of the sandwich Mg–Y alloy keeps at 50Hv for Mg–5Y layer at both sides and increases to 130Hv for the middle layer. Note that, there is a middle value (about 90Hv) between Mg–11Y and Mg–5Y layers. It seems that the hardness decreases gradually instead of steeply falls in the interface transition region marked by yellow rectangle, which might be caused by the interface effect.

The microstructure of the interface transition region is clearly demonstrated by HAADF-STEM image (Fig. 3a). β′ phase is frequently observed in the aged Mg–Y alloy, which is proposed to have a base-cantered orthorhombic structure. The lattice parameters of β′ phase are a = 0.6418 nm, b = 2.2232 nm, c = 0.5210 nm. The stoichiometric of β′ precipitates is Mg_7Y [29,30]. The density of β′ phase decreases gradually in the transition region from Mg–11Y layer to Mg–5Y layer, as shown in Fig. 3b, c and d, respectively. Especially, few β′ phase can be found in Fig. 3d. The interfacial transition region formed, because of the different concentration of Y from Mg–11Y to Mg-5 Y. Due to the significant driving force of thermal dynamics, Y is tended to diffuse from higher concentration region (Mg–11Y) to the lower one (Mg–5Y). Moreover, a high-speed diffusion is achieved in the HPTed sample, because the deformation induced defects are used to become the diffusion channels for alloying elements [8,31]. So, the precipitation strengthening causes the linear decent of hardness in the transition region. In addition, Fig. 3e displays the concentration of Y element in the interface transition region measured along the orange line in Fig. 3a. The values of Y concentration marked by point I-IV is 9.68%, 7.22%, 6.90% and 5.63%, respectively. It dedicates that the concentration of Y decreases gradually in the interface transition region, which is also consist with the trend of hardness from Mg–11Y layer to Mg–5Y layer.

From the abovementioned, a sandwich Mg–Y alloy is produced by sandwiching a Mg–11Y layer between two Mg–5Y layers. After aging treatment, the Mg–11Y layer in the middle transfers to hard zone, and the Mg–5Y layers in both sides transfer to soft zones. This sandwich structure is satisfied with the principle of heterogeneous materials. The interface transition region between hard and soft zone shows a gradient structure of Y concentration and precipitation, which results in the same trend of hardness.

Fig. 4 shows the mechanical properties of heterogeneous Mg–Y, homogeneous (homo) Mg–5Y and Mg–11Y alloys. Fig. 4a and b are the tensile engineering stress-strain curves and the true stress-strain curves, respectively. The yield strength for heterogeneous sandwich Mg–Y, homogeneous Mg–5Y and Mg–11Y alloys are measured as 182 MPa, 81 MPa and 272 MPa, respectively. While their uniform elongations are 6.1%, 17.4% and none, respectively. The yield strength of heterogeneous sandwich Mg–Y alloy is 2.25 times that of homogeneous Mg–5Y alloy, and the uniform elongation also increases greatly compared to homogeneous Mg–11Y alloy. Here, the sandwich Mg–Y alloy attains an enhanced strength-plasticity synergy, which is attributed to hetero-deformation induced (HDI) strengthening and work hardening [32]. The soft zones (Mg–5Y layer) need to deform together with the neighboring hard zone (Mg–11Y layer) and, therefore, cannot plastically deform freely. The strain at the zone interface needs to be continuous, although the soft zone will typically accommodate more strains since they are plastically deforming. Therefore, there will be a plastic strain gradient in the soft zone near the zone interface. This strain gradient needs to be accommodated by geometrically necessary dislocations or deformation twins, which will make the soft phase appear stronger [13, 33,34], leading to synergetic strengthening to increase the global measured yield strength of the heterogeneous material [35]. Fig. 4c shows the strain hardening-true strain curves. The work hardening rate of heterogeneous sandwich Mg–Y is higher than the other two materials, mostly due to HDI work hardening between soft and hard zone in heterogeneous materials [32]. In addition, the interface transition region

Table 1
Initial thickness and structures of three groups of HPT samples.

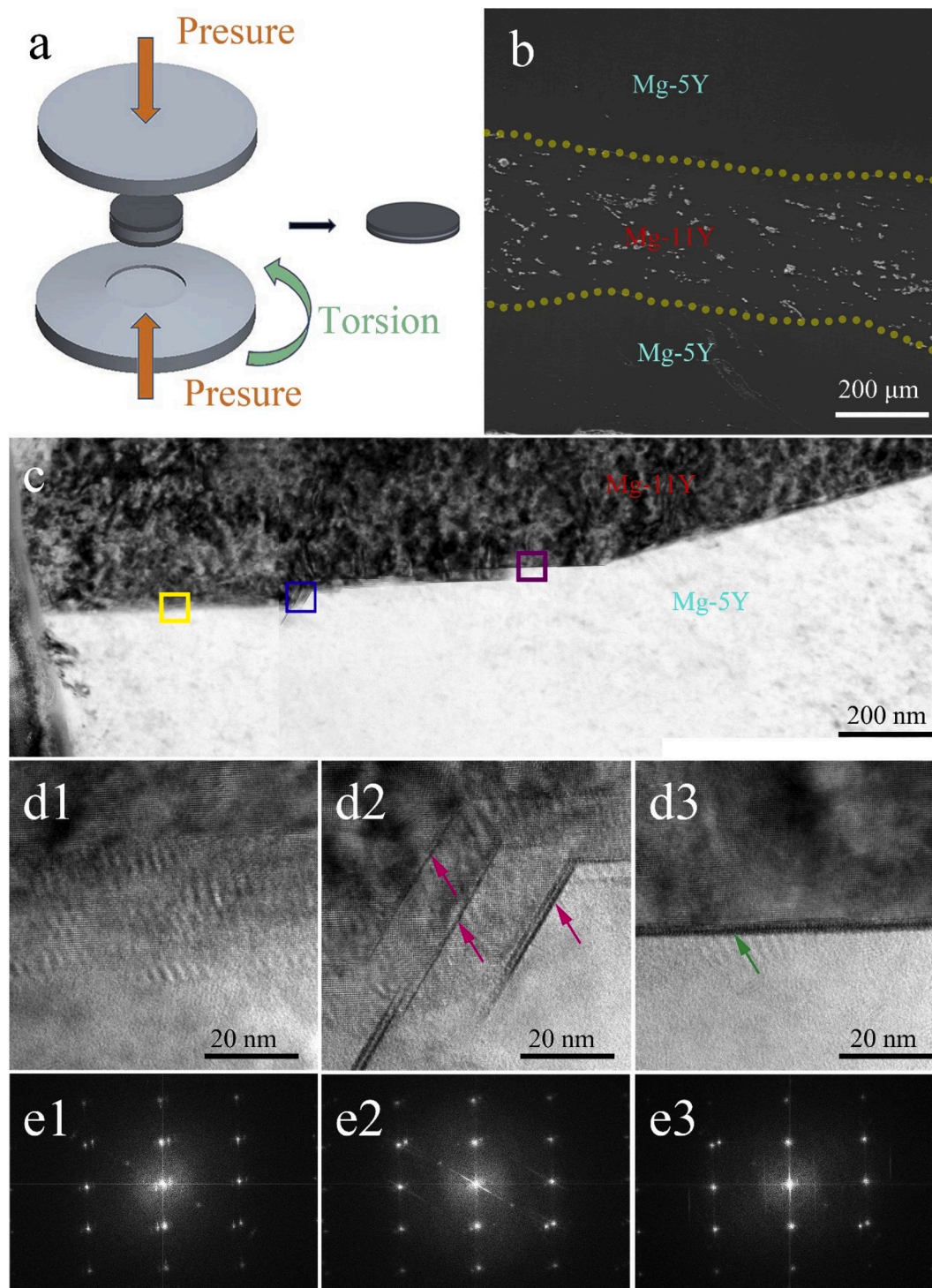| Sandwich Mg–Y	Homogeneous Mg–5Y	Homogenous Mg–11Y
Mg–5Y 0.8 mm Mg–11Y 1.6 mm Mg–5Y 0.8 mm	3.2 mm	3.2 mm

Fig. 1. (a) The diagram of HPT process; (b) SEM image of cross section of sandwich Mg–Y; (c) the bright-field TEM image of the interface; (d1)-(d3) the HRTEM and (e1)-(e3) corresponding FFT patterns of the yellow, blue and purple box in (c), respectively. (For interpretation of the references to colour in this figure legend, the reader is referred to the Web version of this article.)

can enlarge the interface effect between the hard and soft zone, which will further increase the yield strength and HDI work hardening.

In summary, HPT followed by solution and aging treatment was used to produce heterogeneous Mg–Y alloys by sandwiching a hard layer with precipitates and two soft layers with free precipitates. The sandwich Mg–Y alloy attains an enhanced strength-plasticity synergy. Specially, the interface transition region shows a gradient distribution of Y concentration and precipitates, which enlarge the interface effect between

the hard and soft zone. It will further increase the yield strength and HDI work hardening.

Declaration of competing interest

The authors declare that they have no known competing financial interests or personal relationships that could have appeared to influence the work reported in this paper.
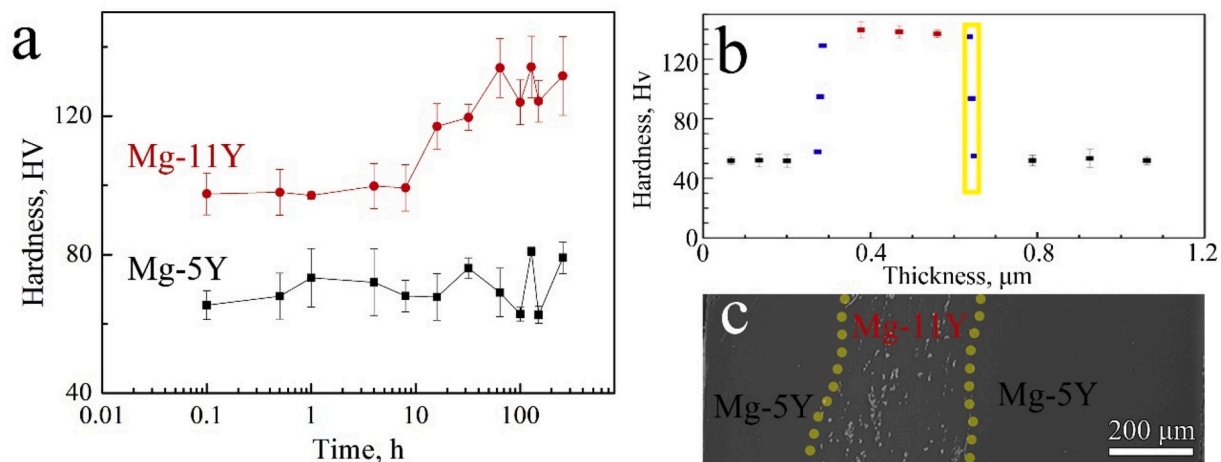
Fig. 2. (a) Age-hardening response of Mg–5Y and Mg–11Y at 200 °C for 256 h; (b) the Vickers hardness of cross section of aged sandwich Mg–Y; (c) the SEM image of testing cross section of aged sandwich Mg–Y.
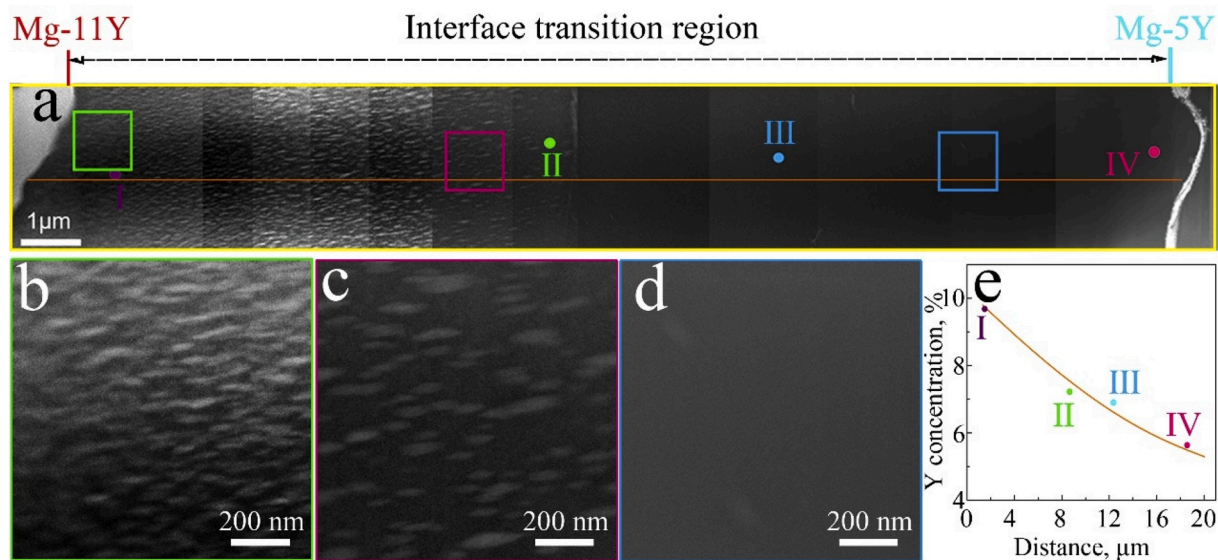

Fig. 3. (a) The HAADF image of the interface transition region of the yellow box in fig. 2b; (b), (c) and (d) are the HAADF images of the green, pink and blue box in (a), respectively; (e) the Y concentration along the orange line in (a) from Mg–11Y to Mg–5Y in the region. (For interpretation of the references to colour in this figure legend, the reader is referred to the Web version of this article.)
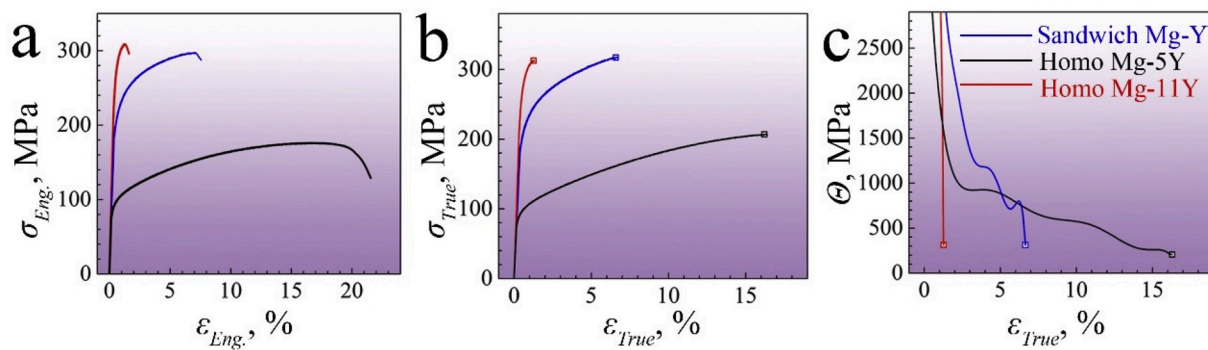

Fig. 4. Tensile properties for the aged sandwich Mg–Y, homogeneous (homo) Mg–5Y and homogeneous (homo) Mg–11Y. (a) Engineering stress-strain curves; (b) True stress-strain curves; (c) Strain hardening-true strain curves.

Acknowledgement

References

[1] B.C. Suh, M.S. Shim, K.S. Shin, N.J. Kim, Current issues in magnesium sheet alloys: where do we go from here? Scripta Mater. 84 (2014) 1–6.
[2] J.F. Nie, Precipitation and hardening in magnesium alloys, Metall. Mater. Trans. 43 (2012) 3891–3939.
[3] T.M. Pollock, Weight loss with magnesium alloys, Science 328 (2010) 986–987.
[4] H. Zhou, H.Y. Ning, X.L. Ma, D.D. Yin, L.R. Xiao, X.C. Sha, Y.D. Yu, Q.D. Wang, Y. S. Li, Microstructural evolution and mechanical properties of Mg-9.8Gd-2.7Y-0.4Zr alloy produced by repetitive upsetting, J. Mater. Sci. Technol. 34 (2018) 1067–1075.
[5] H. Zhou, Q.D. Wang, B. Ye, W. Guo, Hot deformation and processing maps of as-extruded Mg-9.8Gd-2.7Y-0.4Zr Mg alloy, Mater. Sci. Eng., A 576 (2013) 101–107.
[6] L.R. Xiao, Y. Cao, S. Li, H. Zhou, L. Mao, X.C. Sha, Q.D. Wang, Y.T. Zhu, X.D. Han, The formation mechanism of a novel interfacial phase with high thermal stability in a Mg-Gd-Y-Ag-Zr alloy, Acta Mater. 162 (2019) 214–225.
[7] H. Zhou, G.M. Cheng, X.L. Ma, W.Z. Xu, S.N. Mathaudhu, Q.D. Wang, Y.T. Zhu, Effect of Ag on interfacial segregation in Mg-Gd-Y-(Ag)-Zr alloy, Acta Mater. 95 (2015) 20–29.
[8] L.R. Xiao, X.F. Chen, Y. Cao, H. Zhou, X.L. Ma, D.D. Yin, B. Ye, X.D. Han, Y.T. Zhu, Solute segregation assisted nanocrystallization of a cold-rolled Mg-Ag alloy during annealing, Scripta Mater. 177 (2020) 69–73.
[9] S.M. He, X.Q. Zeng, L.M. Peng, X. Gao, J.F. Nie, W.J. Ding, Microstructure and strengthening mechanism of high strength Mg-10Gd-2Y-0.5Zr alloy, J. Alloys Compd. 427 (2007) 316–323.
[10] J.C. Li, Z.L. He, P.H. Fu, Y.J. Wu, L.M. Peng, W.J. Ding, Heat treatment and mechanical properties of a high-strength cast Mg-Gd-Zn alloy, Mater. Sci. Eng., A 651 (2016) 745–752.
[11] W. Rong, Y. Zhang, Y.J. Wu, Y.L. Chen, T. Tang, L.M. Peng, D.Y. Li, Fabrication of high-strength Mg-Gd-Zn-Zr alloys via differential-thermal extrusion, Mater. Char. 131 (2017) 380–387.
[12] X.L. Wu, Y.T. Zhu, Heterogeneous materials: a new class of materials with unprecedented mechanical properties, Mater. Res. Lett. 5 (2017) 527–532.
[13] X.L. Wu, M.X. Yang, F.P. Yuan, G.L. Wu, Y.J. Wei, X.X. Huang, Y.T. Zhu, Heterogeneous lamella structure unites ultrafine-grain strength with coarse-grain ductility, Proc. Natl. Acad. Sci. Unit. States Am. 112 (2015) 14501–14505.
[14] B. Gao, X.F. Chen, Z.Y. Pan, J.S. Li, Y. Ma, Y. Cao, M.P. Liu, Q.Q. Lai, L.R. Xiao, H. Zhou, A high-strength heterogeneous structural dual-phase steel, J. Mater. Sci. 54 (2019) 12898–12910.
[15] H. Zhou, C.X. Huang, X.C. Sha, L.R. Xiao, X.L. Ma, H.W. Hoppel, M. Goken, X. L. Wu, K. Ameyama, X.D. Han, Y.T. Zhu, In-situ observation of dislocation dynamics near heterostructured interfaces, Mater. Res. Lett. 7 (2019) 376–382.
[16] J.S. Li, B. Gao, Z.W. Huang, H. Zhou, Q.Z. Mao, Y.S. Li, Design for strength-ductility synergy of 316L stainless steel with heterogeneous lamella structure through medium cold rolling and annealing, Vacuum 157 (2018) 128–135.
[17] C. Xu, M.Y. Zheng, S.W. Xu, K. Wu, E.D. Wang, S. Kamado, G.J. Wang, X.Y. Lv, Ultra high-strength Mg-Gd-Y-Zn-Zr alloy sheets processed by large-strain hot rolling and ageing, Mater. Sci. Eng., A 547 (2012) 93–98.
[18] H. Zhou, W.Z. Xu, W.W. Jian, G.M. Cheng, X.L. Ma, W. Guo, S.N. Mathaudhu, Q. D. Wang, Y.T. Zhu, A new metastable precipitate phase in Mg-Gd-Y-Zr alloy, Philos. Med. 94 (2014) 2403–2409.
[19] X.C. Sha, L.R. Xiao, X.F. Chen, G.M. Cheng, Y.D. Yu, D.D. Yin, H. Zhou, Atomic structure of γ″ phase in Mg-Gd-Y-Ag alloy induced by Ag addition, Philos. Med. 99 (2019) 1957–1969.
[20] K. Wu, H. Chang, E. Maawad, W.M. Gan, H.G. Brokmeier, M.Y. Zheng, Microstructure and mechanical properties of the Mg/Al laminated composite fabricated by accumulative roll bonding (ARB), Mater. Sci. Eng., A 527 (2010) 3073–3078.
[21] X.L. Ma, C.X. Huang, W.Z. Xu, H. Zhou, X.L. Wu, Y.T. Zhu, Strain hardening and ductility in a coarse-grain/nanostructure laminate material, Scripta Mater. 103 (2015) 57–60.
[22] X.L. Ma, C.X. Huang, J. Moering, M. Ruppert, H.W. Höppel, M. Göken, J. Narayan, Y.T. Zhu, Mechanical properties of copper/bronze laminates: role of interfaces, Acta Mater. 116 (2016) 43–52.
[23] T. Nizolek, I. Beyerlein, N. Mara, J. Avallone, T. Pollock, Tensile behavior and flow stress anisotropy of accumulative roll bonded Cu-Nb nanolaminates, Appl. Phys. Lett. 108 (2016), 051903.
[24] X.F. Chen, L.R. Xiao, Z.G. Ding, W. Liu, Y.T. Zhu, X.L. Wu, Atomic segregation at twin boundaries in a Mg-Ag alloy, Scripta Mater. 178 (2020) 193–197.
[25] P.V. Liddicoat, X.Z. Liao, Y.H. Zhao, Y.T. Zhu, M.Y. Murashkin, E.J. Lavernia, R. Z. Valiev, S.P. Ringer, Nanostructural hierarchy increases the strength of aluminum alloys, Nat. Commun. 1 (2010) 63.
[26] Y. Liu, M.P. Liu, X.F. Chen, Y. Cao, H.J. Roven, M. Murashkin, R.Z. Valiev, H. Zhou, Effect of Mg on microstructure and mechanical properties of Al-Mg alloys produced by high pressure torsion, Scripta Mater. 159 (2019) 137–141.
[27] X.T. Fang, G.Z. He, C. Zheng, X.L. Ma, D. Kaoumi, Y.S. Li, Effect of heterostructure and hetero-deformation induced hardening on the strength and ductility of brass, Acta Mater. 186 (2020) 644–655.
[28] W. Jiang, H. Zhou, Y. Cao, J.F. Nie, Y.S. Li, Y.H. Zhao, M. Kawasaki, T.G. Langdon, Y.T. Zhu, On the heterogeneity of local shear strain induced by high-pressure torsion, Adv. Eng. Mater. 22 (2020) 1900477–1900485.
[29] H. Liu, Y. Gao, J.Z. Liu, Y.M. Zhu, Y. Wang, J.F. Nie, A simulation study of the shape of β′ precipitates in Mg-Y and Mg-Gd alloys, Acta Mater. 61 (2013) 453–466.
[30] E.L.S. Solomon, E.A. Marquis, Deformation behavior of β′ and β″ precipitates in Mg-RE alloys, Mater. Lett. 216 (2018) 67–69.
[31] D. Utt, A. Stukowski, M. Ghazisaeidi, The effect of solute cloud formation on the second order pyramidal to basal transition of c + a edge dislocations in Mg-Y solid solutions, Scripta Mater. 182 (2020) 53–56.
[32] Y.T. Zhu, X.L. Wu, Perspective on hetero-deformation induced (HDI) hardening and back stress, Mater. Res. Lett. 7 (2019) 393–398.
[33] M.X. Yang, Y. Pan, F.P. Yuan, Y.T. Zhu, X.L. Wu, Back stress strengthening and strain hardening in gradient structure, Mater. Res. Lett. 4 (2016) 145–151.
[34] L. Li, S.Z. Wang, L.R. Xiao, X.F. Chen, K. Wei, H.Y. Ning, Y.D. Yu, D.D. Yin, H. Zhou, Atomic-scale three-dimensional structural characterisation of twin interface in Mg alloys, Philo. M, 2020, https://doi.org/10.1080/09500839.2020.1774935.
[35] X.L. Wu, P. Jiang, L. Chen, J.F. Zhang, F.P. Yuan, Y.T. Zhu, Synergetic strengthening by gradient structure, Mater. Res. Lett. 2 (2014) 185–191.